On the effects of nonequilibrium on the subgrid-scale stresses

Ugo Piomelli
Department of Mechanical Engineering, University of Maryland, College Park, Maryland 20742

Gary N. Coleman and John Kim
Department of Mechanical and Aerospace Engineering, University of California, Los Angeles, California 90095-1597

(Received 17 December 1996; accepted 17 April 1997)

An *a priori* study of the subgrid-scale (SGS) stresses and dissipation in two nonequilibrium, wall-bounded flows is carried out. The velocity fields were computed by direct simulations of two- and three-dimensional boundary layers obtained, respectively, by a sudden change in the Reynolds number and by an impulsive motion in the spanwise direction of the lower wall of a plane channel in fully developed turbulent flow conditions. Several realizations of the transient period of the flow were examined. The SGS stresses react to the imposition of the secondary shear more rapidly than the large-scale ones, and return to equilibrium before the resolved stresses do. In general, the subgrid scales are less sensitive than the large ones to the near-wall and nonequilibrium effects. Scale-similar and dynamic models appear well-suited to reproduce the correlation between resolved Reynolds stress production and events with significant production of SGS energy. © *1997 American Institute of Physics.* [S1070-6631(97)01208-7]

I. INTRODUCTION

Large-eddy simulations (LES) of the Navier–Stokes equations are based on the assumption that the small, subgrid scales of motion are more universal than the large, energy-carrying ones, less affected by the boundary conditions, and, therefore, easier to model. Since in LES only the largest structures are computed, coarser grids can be used than in direct simulations, and higher Reynolds number flows can be studied at a fraction of the expense. Moreover, the modeling of the small scales in principle is simpler than the modeling of all the scales of motions required by Reynolds-averaged (RANS) calculations, and, therefore, better accuracy can be achieved, especially in three-dimensional flows for which most turbulence models (especially two-equation models) are known to be inadequate.

Since the small scales tend to be more homogeneous and isotropic than the large ones, simple models should be able to describe their physics fairly accurately. Furthermore, since the subgrid-scale (SGS) stresses are a small fraction of the total stresses, modeling errors should not affect the overall accuracy of the results as much as in the Reynolds-averaged turbulence modeling approach. For these reasons, most subgrid scale models in use presently are eddy-viscosity models that relate the subgrid-scale stresses, τ_{ij}, to the large-scale strain-rate tensor $\overline{S}_{ij}$. The eddy viscosity is given by the product of a length scale, ℓ, and a velocity scale, q_{sgs}. Since the most active unresolved scales are those closest to the cutoff, the natural length scale in LES modeling is the filter width, which is representative of the size of the smallest resolved structure in the flow, and is typically proportional to the grid size. The velocity scale is usually taken to be the square root of the trace of the SGS stress tensor, $q_{sgs}^2=\tau_{kk}$. To determine q_{sgs}^2 in most cases the equilibrium assumption is exploited to obtain an algebraic model for the eddy viscosity.[1]

The Smagorinsky model can be derived[2] based on the observation that the small scales of motion have shorter time scales than the large, energy-carrying eddies; for this reason, it can be assumed that they adjust more rapidly than the large scales to perturbations, and recover equilibrium nearly instantaneously. Under this assumption, the transport equation for q_{sgs}^2 reduces to $-\tau_{ij}\overline{S}_{ij}=\varepsilon_v$, where $-\tau_{ij}\overline{S}_{ij}$ is the production, and ε_v the viscous dissipation, of SGS energy. The negative of the production term, $\varepsilon_{sgs}=\tau_{ij}\overline{S}_{ij}$, is often referred to as the ''SGS dissipation,'' since it also represents the dissipation of resolved energy by the SGS stresses. This balance, together with the definition of the eddy viscosity, can be used to obtain the velocity scale.

The equilibrium assumption implies inertial range dynamics: energy is generated at the large-scale level and transmitted to smaller and smaller scales, where the viscous dissipation takes place. Very little testing of the applicability of this assumption to the small scales of turbulence is available. It is well known that in most flows of interest the large scales are not in equilibrium: Smith and Yakhot[3] studied the short-time behavior of the eddy viscosity in the Reynolds-averaged framework, and found that $\mathcal{K}-\varepsilon$ models do not predict the correct response of the eddy viscosity if homogeneous isotropic turbulence is suddenly subjected to a perturbation (system rotation or shear, for instance). They conjecture that SGS models will suffer from the same shortcomings unless a short-time correction is applied. The fact that the Smagorinsky SGS model, applied to the study of homogeneous turbulence suddenly subjected to shear (Bardina *et al.*[4]) gave results in good agreement with the theory of Smith and Yakhot,[3] however, indicates that the small scales tend to equilibrium faster than the large ones, and thus satisfy the equilibrium assumption better than the large scales do. This suggests that, at least in this flow, as long as the correct nonequilibrium response of the large scales is captured, the overall development may be predicted with satisfactory accuracy even by equilibrium-based SGS models. In more

 1070-6631/97/9(9)/2740/9/$10.00

complex flows, in which extra strains, backscatter, intermittency, and other phenomena play a role, it is not known whether the small scales would still be represented adequately by equilibrium-based subgrid-scale models.

The purpose of this paper is to study the physical behavior of the subgrid scales of motion in situations of strong perturbation from equilibrium by *a priori* testing. Two cases will be studied: The first is a fully developed plane channel flow in which the viscosity is suddenly decreased to accelerate the flow, which reaches equilibrium at a higher Reynolds number; the second, a three-dimensional, shear-driven boundary layer,[5] obtained by moving the lower wall of a fully developed plane channel flow in the spanwise direction. Both flows are initially equilibrium flows that approach another equilibrium state, and thus allow comparison of the response of both large and subgrid scales to the perturbation, and their return to equilibrium.

Furthermore, the performance of several models will be compared. The models chosen are the Smagorinsky model,[1] the dynamic eddy-viscosity model,[6,7] and two scale-similar models.[8,9] Both the Smagorinsky and the dynamic model are eddy-viscosity models; the model coefficient in the former is set *a priori*, while in the latter it is adjusted according to the energy content of the simulation. Thus the dynamic model should be able to adjust more rapidly than the Smagorinsky model to the perturbations. Scale-similar models use the smallest resolved scales to parametrize the unresolved ones. They are based on the hypothesis that the most important interactions between resolved and unresolved scales occur between the eddies closest to the cutoff wave number. This dependence on the model on the smallest resolved scales will also be shown to have beneficial effects for the prediction of the response of the SGS stresses to perturbations.

In the next section the governing equations and the mathematical approach will be presented. The results of the *a priori* test will be presented is Sec. III. Some conclusions will be drawn in the last section.

II. PROBLEM FORMULATION

A. Governing equations

In LES dependent flow variables are divided into a grid-scale (GS) part and a subgrid-scale (SGS) part by the filtering operation

$$\overline{f}(\mathbf{x})=\int_D f(\mathbf{x}')G(\mathbf{x},\mathbf{x}')d\mathbf{x}', \tag{1}$$

where D is the computational domain, and G is the filter function. The application of this operation to the continuity and Navier–Stokes equations yields the equations that govern the evolution of the large, energy-carrying scales of motion:

$$\frac{\partial \overline{u}_i}{\partial t}+\frac{\partial}{\partial x_j}(\overline{u_i u_j})=-\frac{1}{\rho}\frac{\partial \overline{p}}{\partial x_i}-\frac{\partial \tau_{ij}}{\partial x_j}+\nu\frac{\partial^2 \overline{u}_i}{\partial x_j \partial x_j}, \tag{2}$$

$$\frac{\partial \overline{u}_i}{\partial x_i}=0, \tag{3}$$

where x (or x_1) is the streamwise direction, y (or x_2) the wall–normal direction, and z (or x_3) the spanwise direction; u, v, and w (or u_1, u_2, and u_3) are the velocity components in the coordinate directions. The effect of the small scales appears in the SGS stress term, $\tau_{ij}=\overline{u_i u_j}-\overline{u}_i\overline{u}_j$, which must be modeled.

B. Subgrid-scale stress models

In the past, two main types of models have been used to parametrize the SGS stresses: eddy viscosity and scale-similar models. Eddy-viscosity models represent the anisotropic part of the SGS stress tensor as

$$\tau_{ij}-\frac{\delta_{ij}}{3}\tau_{kk}=-2\nu_T\overline{S}_{ij}, \tag{4}$$

where ν_T is the eddy viscosity and $\overline{S}_{ij}$ is the large-scale strain rate tensor

$$\overline{S}_{ij}=\frac{1}{2}\left(\frac{\partial \overline{u}_i}{\partial x_j}+\frac{\partial \overline{u}_j}{\partial x_i}\right). \tag{5}$$

The assumption that $-\tau_{ij}\overline{S}_{ij}=\varepsilon_v$, where

$$\varepsilon_v=\left(\overline{\frac{\partial u_i}{\partial x_j}\frac{\partial u_i}{\partial x_j}}-\frac{\partial \overline{u}_i}{\partial x_j}\frac{\partial \overline{u}_i}{\partial x_j}\right), \tag{6}$$

allows the eddy viscosity to be written as[1]

$$\nu_T=(C_S\Delta)^2|\overline{S}|, \tag{7}$$

where $|\overline{S}|=(2\overline{S}_{ij}\overline{S}_{ij})^{1/2}$, Δ is the (grid-scale) filter width, and the Smagorinsky constant, C_S, can be determined by integrating the vorticity spectrum function over all the unresolved wave numbers.[2] In practice, the value of the constant is substantially reduced in the presence of shear, and van Driest[10] damping is used to account for near-wall effects; the eddy viscosity thus becomes

$$\nu_T=[C_S\Delta(1-e^{-y^+/25})]^2|\overline{S}|, \tag{8}$$

where $y^+=y_w u_\tau/\nu$, y_w is the distance from the wall, and $C_s\simeq 0.065-0.1$.

Recently, dynamic models have been introduced that adjust the coefficient locally and instantaneously from the energy content of the smallest resolved scales.[6] These are generally Smagorinsky-like models in which the coefficient C is determined based on the energy content of the smallest resolved scales of motion. In this work, the plane-averaged formulation,[7] which has been applied successfully to the simulation of transitional and turbulent plane channel flows[6,11] will be used, in which the SGS stresses are given by (4), with $\nu_T=C\Delta^2|\overline{S}|$, and

$$C=-\frac{1}{2}\frac{\langle \mathscr{L}_{ij}M_{ij}\rangle}{\langle M_{mn}M_{mn}\rangle}, \tag{9}$$

where $\langle\cdot\rangle$ denotes an average taken over planes parallel to the wall, $\mathscr{L}_{ij}=\widehat{\overline{u}_i\overline{u}_j}-\hat{\overline{u}}_i\hat{\overline{u}}_j$ are the resolved turbulent stresses, $M_{ij}=\hat{\Delta}^2|\hat{\overline{S}}|\hat{\overline{S}}_{ij}-\Delta^2\widehat{|\overline{S}|\overline{S}_{ij}}$, and a hat denotes the application of a filter with width $\hat{\Delta}=2\Delta$.

Scale similar models also use the energy content of the smallest resolved scales of motion to predict the behavior of the SGS stresses. In this work, two such models will be tested, the one originally developed by Bardina *et al.*:[8]

$$\tau_{ij}=\overline{\overline{u_i u_j}}-\overline{\overline{u}_i\overline{u}_j} \tag{10}$$

and the one recently proposed by Liu *et al.*:[9]

$$\tau_{ij}=C_L\mathscr{L}_{ij}; \tag{11}$$

Liu *et al.*[9] recommended a value $C_L=0.45$. The coefficient can also be adjusted dynamically.

C. *A priori* tests

In *a priori* tests the resolved velocity fields obtained from direct simulations of the Navier–Stokes equations are filtered explicitly according to (1) to yield the exact SGS quantities of interest. Two filter functions are considered in this study: the sharp cutoff filter in Fourier space and the box (or tophat) filter in physical space. The sharp cutoff filter is best defined in Fourier space as:

$$g(k)=\int_D G(x')e^{-ikx'}dx'=\begin{cases}1, & \text{if } k\leqslant\pi/\Delta,\\ 0, & \text{otherwise,}\end{cases} \tag{12}$$

while the box (or top hat) filter is

$$G(x)=\begin{cases}1/\Delta, & \text{if } |x|\leqslant\Delta/2,\\ 0, & \text{otherwise.}\end{cases} \tag{13}$$

Three DNS databases were used in this work: the first is the DNS of a two-dimensional plane channel flow at $Re_\tau=180$ (based on friction velocity u_τ and channel half-width δ), computed using a pseudo-spectral code with $128\times97\times128$ grid points and a computational domain of $4\pi\delta\times2\delta\times4\pi\delta/3$. The results of this calculation were shown by Piomelli *et al.*[12] to be in good agreement with the direct numerical simulations (DNS) of Kim *et al.*[13] The accelerating channel case was computed using the same pseudo-spectral code; the flow was started from a steady-state field at $Re_\tau=150$ (based on the initial friction velocity $u_{\tau,o}$ and viscosity ν_o); the Reynolds number was then suddenly increased, and a new equilibrium state was reached at $Re_\tau=225$ at $tu_{\tau,o}/\delta\simeq1.2$.

The shear-driven three-dimensional boundary layer velocity fields were obtained from the calculations by Coleman *et al.*[5] using the spectral code of Kim *et al.*[13] The computational domain was $4\pi\delta\times2\delta\times8\pi\delta/3$ in the streamwise (x_1 or x), wall-normal (x_2 or y), and spanwise (x_3 or z) directions, respectively, and $256\times129\times256$ grid points were used. An impulsive spanwise motion, with magnitude equal to 47% of the initial mean centerline velocity, was applied to the lower wall of a fully developed plane channel flow; the initial condition was obtained from the calculation at Reynolds number $Re_\tau=180$. The flow was allowed to develop until a collateral state (one in which the new direction of the mean velocity is the same at each y) was reached. Notice that, since periodic boundary conditions were used, the boundary layer due to the spanwise motion of the wall grows in time rather than in space.

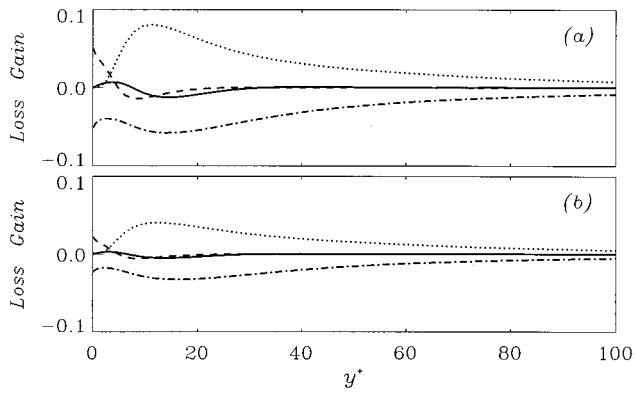

FIG. 1. Terms in the SGS kinetic budget in the two-dimensional plane channel flow, $Re_\tau=180$, normalized by u_τ and ν. Tophat filter. · · · ·, production; - · - · - ·, viscous dissipation; - - -, viscous diffusion; ——, remaining terms. (a) $\Delta_i=4\Delta x_i$; (b) $\Delta_i=2\Delta x_i$.

The exact GS and SGS fields were obtained by filtering the DNS data over the streamwise and spanwise homogeneous directions using different filter types and sizes. A typical test performed using the Fourier cutoff filter employs a filter width $\Delta_i=4\Delta x_i$ (for $i=1$ and 3); for the box filter widths $\Delta_i=2\Delta x_i$ and $\Delta_i=4\Delta x_i$ were used. With these values, the ratio of SGS to total fluctuating energy was 15%–25%, a range representative of actual LES calculations. No significant difference was observed between the results for the two filters.

All the data shown in the following were averaged over several realizations of the flow fields in question, as well as over planes parallel to the wall. Since the expense required to generate ensembles of data in this type of unsteady flows is significant, the sample size in some cases is insufficient to obtain fully converged results. However, the purpose of the *a priori* test is only to supply physical insight into the phenomena that affect the subgrid scales and identify the trends; for this purpose, the sample size is adequate.

Two normalizations will be used: one in which all quantities are made dimensionless using the initial friction velocity $u_{\tau,o}$ and molecular viscosity ν_o. In the other the time-dependent values of the friction velocity u_τ and viscosity ν are used. Quantities made dimensionless by the latter normalizations will be denoted by a prime.

III. RESULTS AND DISCUSSION

A. Plane channel flow

In Fig. 1 the terms in the budget of the SGS kinetic energy $\mathscr{K}_{sgs}=\tau_{kk}/2$ are shown for the two-dimensional plane channel flow as a function of y^+. The assumption that production and dissipation of SGS energy are in balance holds well outside the viscous sublayer ($y^+>30$), and only very near the wall are nonlocal effects important. This is consistent with the finding that, in the core of the flow, dynamic eddy-viscosity models yield a value for the model coefficient close to that obtained using the equilibrium assumption and a Kolmogorov form of the spectrum.[11] It should also be pointed out that in the budget for the total

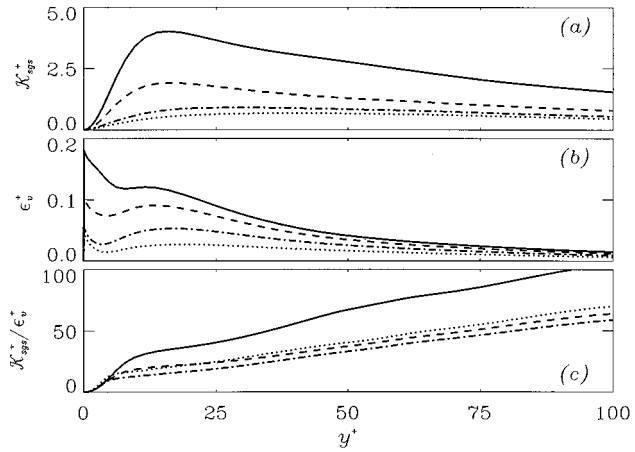

FIG. 2. SGS kinetic energy, viscous dissipation, and eddy turnover time in the two-dimensional plane channel flow, $Re_\tau = 180$, normalized by u_τ and ν. Fourier cutoff filter. ——, $\Delta_i \to \infty$; - - - -, $\Delta_i = 8\Delta x_i$; - · - · - ·, $\Delta_i = 4\Delta x_i$; · · · ·, $\Delta_i = 2\Delta x_i$. (a) SGS kinetic energy; (b) viscous dissipation; (c) $\mathcal{K}^+_{sgs}/\varepsilon^+_v$.

kinetic energy, at this Reynolds number, production and dissipation are not in balance near the wall, where the various diffusion terms are significant;[14] in the outer region the turbulent transport term is not negligible. Only at much higher Reynolds number does behavior like that observed here for the SGS energy become apparent. This point further supports the equilibrium assumption for the small scales.

When homogeneous turbulence is suddenly subjected to mean shear, its short-time response is characterized by a lag between the imposition of the strain and the increase in turbulent kinetic energy due to the increased production. Smith and Yakhot[3] accounted for the lag, within the framework of $\mathcal{K}-\varepsilon$ models, by introducing an exponential correction to the eddy viscosity, which includes a time constant, the eddy turnover time $\tau \sim \mathcal{K}/\varepsilon$. In the context of LES, in which the SGS model only represents the scales smaller than the filter width, a relevant eddy turnover time must be defined in terms of SGS quantities only, and could depend on the filter width. In Fig. 2 such an eddy turnover time, defined in terms of $\mathcal{K}_{sgs}$ and ε_v is shown as a function of distance from the wall for the two-dimensional channel; the Fourier cutoff filter was used. The plane-averaged values ($\Delta_i \to \infty$) are equivalent to long-time averages and thus represent the eddy turnover time relevant to $\mathcal{K}-\varepsilon$ models. Both SGS energy and viscous dissipation decrease as the filter width is decreased; the SGS turnover time is, however, fairly independent of the filter width, and, except very near the wall, is equal to about 50%–60% of the Reynolds-averaged turnover time. While the subgrid scales can be expected to react more rapidly than the largest scales of motion, their response to a perturbation is not instantaneous. Accounting for this adjustment time could improve significantly the accuracy of SGS stress models.

B. Accelerating channel flow

In the accelerating channel flow the perturbation that disrupts the equilibrium state consists of a sudden increase of

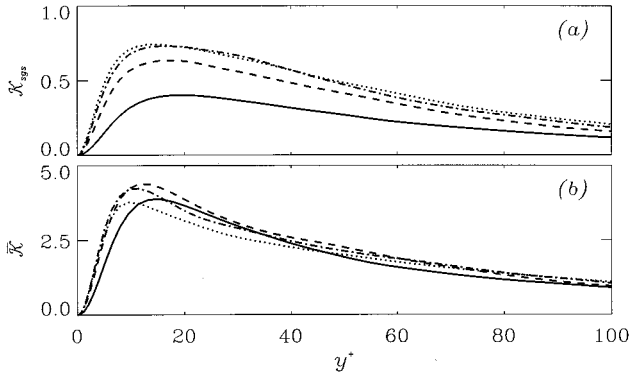

FIG. 3. SGS and large-scale energy, normalized by $u_{\tau,o}$. Accelerating channel flow, top hat filter, $\Delta_i = 2\Delta x_i$. ——, $tu_{\tau,o}/\delta = 0.06$; - - - -, $tu_{\tau,o}/\delta = 0.32$; - · - · - ·, $tu_{\tau,o}/\delta = 0.52$; · · · ·, $tu_{\tau,o}/\delta = 0.70$. (a) SGS energy; (b) large-scale energy.

the Reynolds number. Consequently, one would expect the high-wave-number region of the velocity spectra to fill up, and the small scales should be affected more than the large ones by the perturbation.

In Fig. 3 large-scale and SGS kinetic energy profiles are shown at various times during the transient. While the maximum total kinetic energy, $\overline{\mathcal{K}} + \mathcal{K}_{sgs}$ increases only by 25%, the subgrid-scale energy increases by more than a factor of 2. Similarly, the production of SGS energy (not shown) increases roughly by a factor of 3 during the transient, while the production of large-scale energy at the last time examined ($tu_{\tau,o}/\delta = 0.58$) is only 30% higher than before the perturbation was applied.

If the time-dependent value of the friction velocity is used to normalize the data instead of the initial one, a different trend is observed: the SGS turbulent kinetic energy (Fig. 4) quickly reaches a new equilibrium value (roughly at $tu_{\tau,o}/\delta \simeq 0.3$) and is thereafter nearly independent of time, while the large-scale quantity requires a much longer time to reach a new equilibrium state. This is another strong indication that the small scales tend to adapt to the perturbation much faster than the large scales do, since the former react to

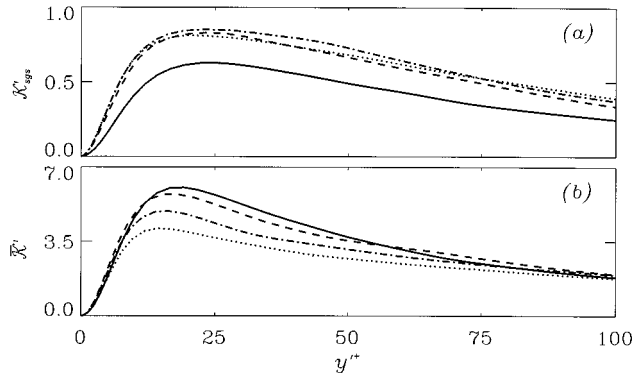

FIG. 4. SGS and large-scale energy normalized by u_τ. Accelerating channel flow, top hat filter, $\Delta_i = 2\Delta x_i$. ——, $tu_{\tau,o}/\delta = 0.06$; - - - -, $tu_{\tau,o}/\delta = 0.32$; - · - · - ·, $tu_{\tau,o}/\delta = 0.52$; · · · ·, $tu_{\tau,o}/\delta = 0.70$. (a) SGS energy; (b) large-scale energy.

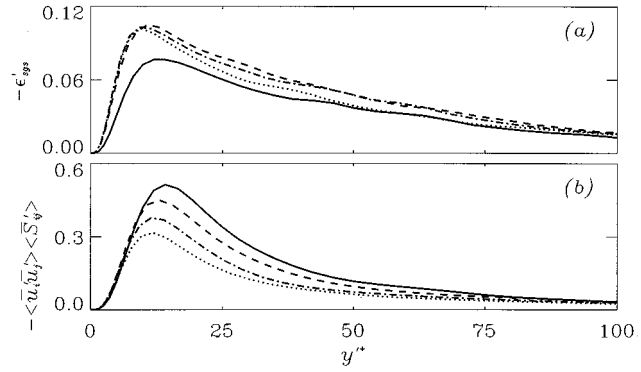

FIG. 5. Production of SGS and large-scale energy, normalized by u_τ and ν. Accelerating channel flow, tophat filter, $\Delta_i = 2\Delta x_i$. ——, $tu_{\tau,o}/\delta = 0.06$; - - - -, $tu_{\tau,o}/\delta = 0.32$; - · - · - ·, $tu_{\tau,o}/\delta = 0.52$; · · · ·, $tu_{\tau,o}/\delta = 0.70$. (a) Production of SGS energy; (b) production of large-scale energy.

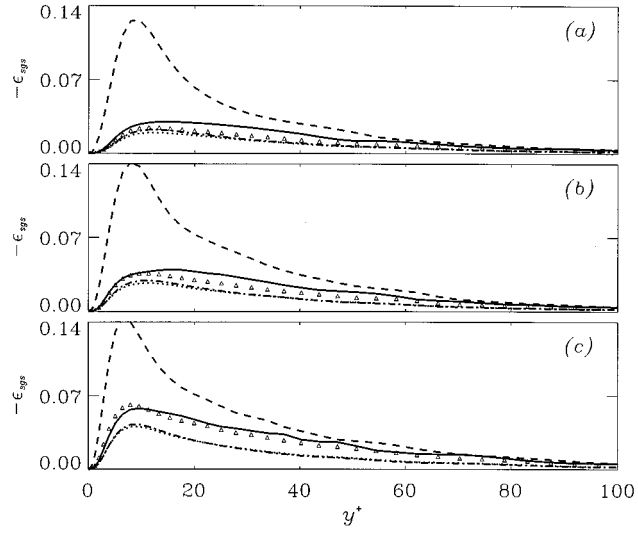

FIG. 7. Wall–normal distribution of the exact and modeled production of SGS energy, normalized by $u_{\tau,o}$ and ν_o. Accelerating channel flow. Tophat filter, $\Delta_i = 2\Delta x_i$. △ Exact; ——, dynamic eddy viscosity model;[6,7] - - - -, Smagorinsky model[1] [Eq. (8)]; - · - · - ·, scale similar model;[9] · · · ·, scale similar model.[8] (a) $tu_{\tau,o}/\delta = 0$; (b) $tu_{\tau,o}/\delta = 0.13$; (c) $tu_{\tau,o}/\delta = 0.32$.

the ''current state'' (represented by the time-dependent velocity scale u_τ) fairly rapidly, whereas the large scales adapt more slowly. The production of SGS and large-scale energy also exhibit a similar trend (Fig. 5).

One of the main purposes of SGS models is to dissipate the correct overall amount of energy from the resolved scales. The total energy drain is the negative of the integral, over the wall-normal direction, of the (time- and plane-averaged) production of SGS energy. The time development of this quantity, together with the integral of the large-scale production, is shown in Fig. 6(b); in Fig. 6(a) the integral of the large-scale and SGS energy is shown. Under the time-dependent normalization (u_τ and ν) the subgrid-scale production and energy do not vary as much as when they are normalized by the initial u_τ and ν, indicating that they are better described by the local state of the turbulence; by contrast, the large-scale quantities vary less when normalized by the initial friction velocity and viscosity.

In Fig. 7 profiles of $-\varepsilon_{sgs}$ are compared with those obtained from several models. The Smagorinsky model not only provides excessive levels of the production throughout the channel, but also does not predict accurately the increase in production that follows the imposition of the perturbation. The time development of the production of SGS energy integrated over the channel height is shown Fig. 8; the integral normalized by its initial value [Fig. 8(a)] indicates that the scale-similar models[8,9] and the dynamic model[6,7] follow the trend more closely. The unnormalized values [shown in Fig. 8(b)] indicate that the scale-similar models tend to underpredict the production of SGS energy, consistent with the findings of Bardina *et al.*,[8] who developed the mixed model, which includes a dissipative as well as a scale-similar part, to overcome this shortcoming.

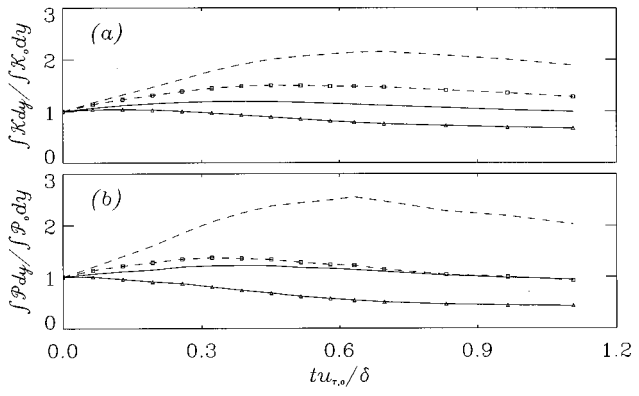

FIG. 6. Time development of the integral of the large-scale and SGS quantities normalized by their initial values. Accelerating channel flow. Tophat filter, $\Delta_i = 2\Delta x_i$. Lines without symbols: quantities normalized by $u_{\tau,o}$ and ν_o; lines with symbols: quantities normalized by u_τ and ν. (a) ——, Large-scale energy; - - - -, SGS energy. (b) ——, Production of large-scale energy; - - - -, production of SGS energy.

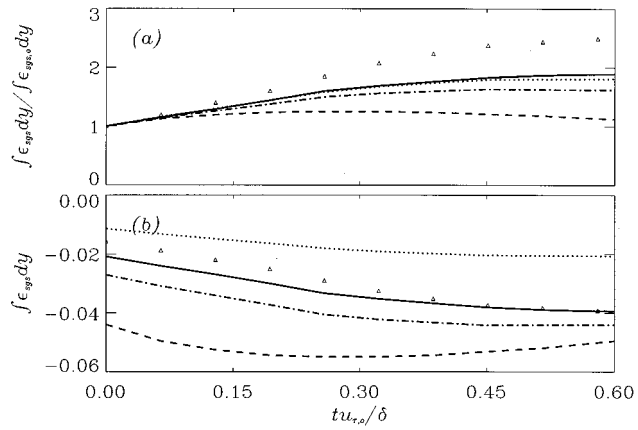

FIG. 8. Time development of the integral of the production of SGS energy. Accelerating channel flow. Tophat filter; $\Delta_i = 2\Delta x_i$. △Exact; ——, dynamic eddy viscosity model;[6,7] - - - -, Smagorinsky model[1] [Eq. (8)]; - · - · - ·, scale similar model;[9] · · · ·, scale similar model.[8] (a) Normalized by its initial value; (b) unnormalized.

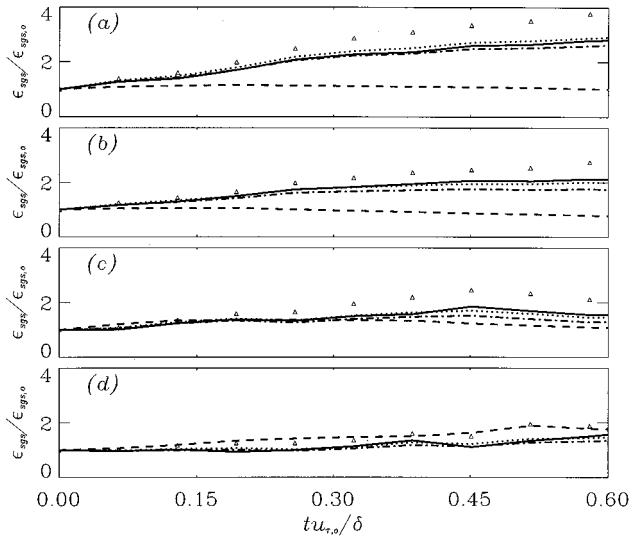

FIG. 9. Time development of exact and modeled production of SGS energy. Accelerating channel flow. Tophat filter, $\Delta_i = 2\Delta x_i$. All quantities are normalized by $u_{\tau,o}$ and ν, and their initial value. △Exact; ——, dynamic eddy viscosity model;[6,7] - - - -, Smagorinsky model[1] [Eq. (8)]; -·-·-· scale similar model;[9] · · · ·, scale similar model.[8] (a) $y^+ = 8$; (b) $y^+ = 13$; (c) $y^+ = 31$; (d) $y^+ = 110$.

The increased production predicted by the Smagorinsky model is particularly significant in the near-wall layer, where the scale-similar and dynamic models predict the response to the perturbation fairly accurately (Fig. 9). In the buffer layer and above the perturbation does not appear to have such a strong effect.

The principal shortcoming of eddy-viscosity models is the fact that the time scale, $|\overline{S}|^{-1}$, is mostly affected by the large scales; thus they do not, in general, respond well to perturbations that affect mostly the small scales. This is the reason for the poor performance of the Smagorinsky model in this flow. The dynamic eddy-viscosity model appears to compensate for this deficiency by adjusting the model coefficient according to the state of the smallest resolved scales; the scale-similar models have a similar behavior. This is evidenced in Fig. 10, in which the development of the kinetic energy spectrum at $y^+ = 13$ is shown. The increase in energy at the high wave numbers is apparent. The scales that contribute most to the resolved turbulent stresses $\mathscr{L}_{ij}$ (to a first approximation, the wave numbers contained between the two ellipses in the figure) also increase significantly during the transient, more so than the largest scales of motion (the contours near the origin), which remain essentially unchanged. Thus it appears that the double filtering operation employed by both dynamic and scale-similar models is beneficial in isolating the scales that most closely represent the smallest scales of motion.

C. Three-dimensional boundary layer

Similar results were obtained from the three-dimensional boundary layer simulation. In this flow the perturbation is applied more gradually, and is also localized in space (at the wall), while the Reynolds number change of the previous flow is felt everywhere. The SGS energy (Fig. 11) can be observed to react more quickly to the imposition of the perturbation than the large-scale energy (especially near the wall), but the phenomenon is not as clear as in the preceding case, due to the local nature of the perturbation.

The more accurate predictions obtained by the dynamic and scale-similar models are evidenced in Figs. 12 and Figs.

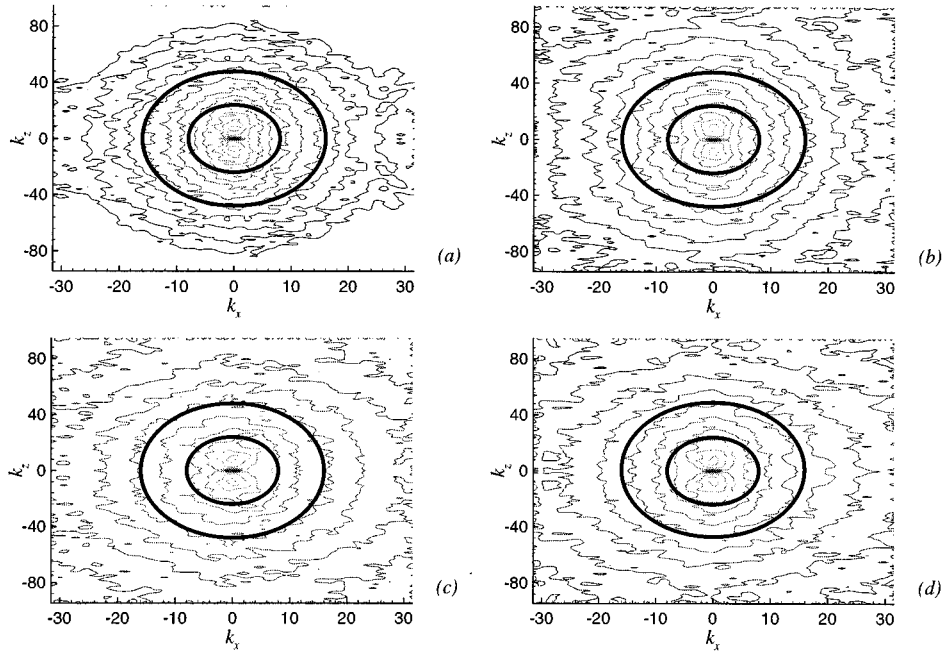

FIG. 10. Kinetic energy spectra (normalized by $u_{\tau,o}$) at $y^+ = 13$. Accelerating channel flow. The contour levels are exponentially spaced between 10^{-7} (black) and 10^0 (grey); the two ellipses roughly correspond to the grid- and test-filter wave numbers. (a) $tu_{\tau,o}/\delta = 0$; (b) $tu_{\tau,o}/\delta = 0.13$; (c) $tu_{\tau,o}/\delta = 0.32$; (d) $tu_{\tau,o}/\delta = 0.58$.

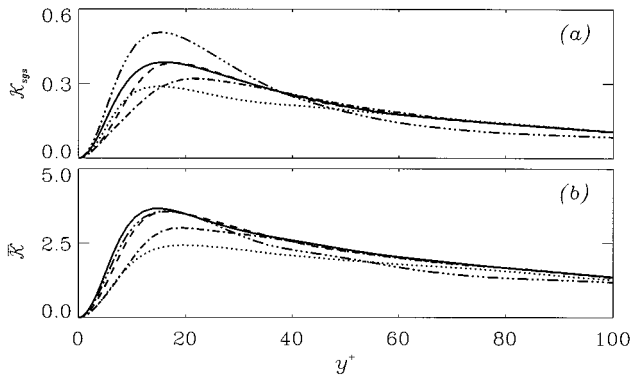

FIG. 11. SGS and large-scale energy, normalized by $u_{\tau,o}$. Three-dimensional boundary layer. Tophat filter, $\Delta_i = 2\Delta x_i$. ——, $tu_{\tau,o}/\delta = 0$; - - - -, $tu_{\tau,o}/\delta = 0.075$; -·-·-·, $tu_{\tau,o}/\delta = 0.15$; · · · ·, $tu_{\tau,o}/\delta = 0.30$, — · · ·—, $tu_{\tau,o}/\delta = 0.75$. (a) SGS energy; (b) large-scale energy.

13, in which, respectively, the integrated production of SGS energy, $-\varepsilon_{sgs}$, and its development at several wall-normal locations are shown. The Smagorinsky model initially predicts increased production in the near-wall region (instead of the reduced dissipation that is observed in the DNS data), reflecting the imposition of the transverse shear $\partial W/\partial y$, which gives an increase in the eddy viscosity. The other models follow the correct trend, because the smallest resolved scales are used to evaluate the coefficient. This is confirmed by the kinetic energy spectra (Fig. 14), which show features similar to those observed in the accelerating channel flow. The scales included between the two filters behave in a manner very similar to the unresolved scales.

Another useful feature of scale-similar models is that they parametrize the unresolved scales in terms of the smallest resolved ones, which have been shown[15–17] to be responsible for most of the energy transfer between resolved and unresolved scales. Piomelli and co-workers[12] observed significant correlation between regions of high Reynolds stress and production of SGS energy. This correlation can be observed in the present data as well. Figure 15 compares contours of total production and production of SGS energy. A strong correlation can be observed between the exact

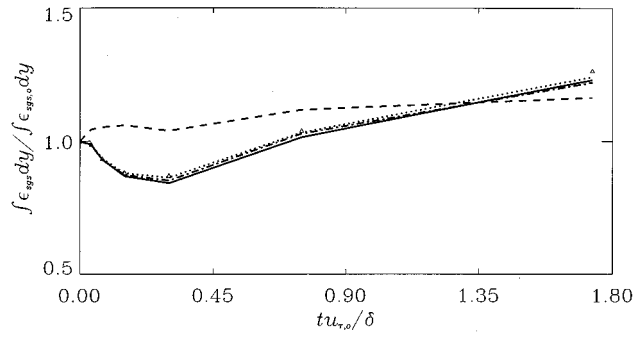

FIG. 12. Time development of the integral of the production of SGS energy. Three-dimensional boundary layer. Tophat filter, $\Delta_i = 2\Delta x_i$. All quantities are normalized by $u_{\tau,o}$ and ν, and their initial value. △Exact; ——, dynamic eddy viscosity model;[6,7] - - - -, Smagorinsky model[1] [Eq. (8)]; -·-·-·, scale similar model;[9] · · · ·, scale similar model.[8]

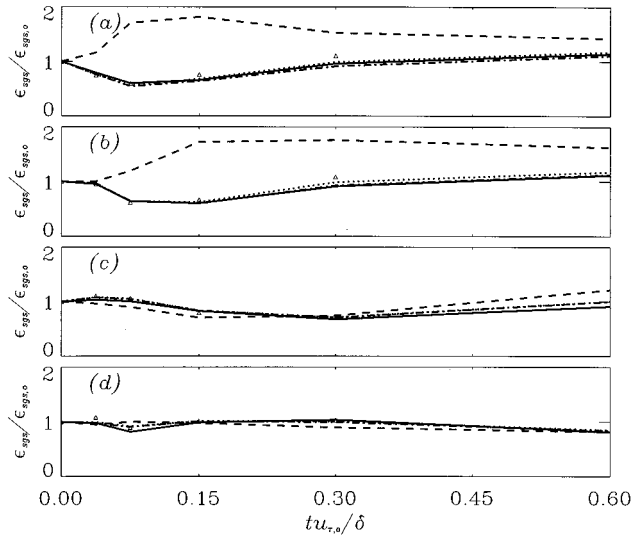

FIG. 13. Time development of exact and modeled production of SGS energy. Three-dimensional boundary layer. Tophat filter, $\Delta_i = 2\Delta x_i$. All quantities are normalized by $u_{\tau,o}$ and ν, and their initial value. △Exact; ——, dynamic eddy viscosity model;[6,7] - - - -, Smagorinsky model[1] [Eq. (8)]; -·-·-·, scale similar model;[9] · · · ·, scale similar model.[8] (a) $y^+ = 8$; (b) $y^+ = 13$; (c) $y^+ = 31$; (d) $y^+ = 110$.

$-\varepsilon_{sgs}$ and the total production; this correlation is reproduced well by the scale-similar model, but less accurately by the eddy viscosity model, which, being statistical in nature, cannot be expected to be as successful in reproducing deterministic events of the type responsible for the distribution of $-\varepsilon_{sgs}$.

IV. CONCLUSIONS

The velocity fields obtained from the direct simulation of two nonequilibrium flows, an accelerating channel flow and a three-dimensional boundary layer, were studied to determine the response to perturbations of the subgrid scales of motion, and their return to equilibrium.

The subgrid scales have a reduced turnover time compared with the resolved scales of motion. The fact that this time-scale is not a small fraction of the large-eddy turnover time is partly due to the low Reynolds number of the DNS data used in the present *a priori* study; in such situations, the strongest interactions between resolved and unresolved scales occur between structures within two octaves of the cutoff wave number. At high Reynolds numbers, when widely separated scales are present, this local interaction may be less dominant, but is still expected to be relevant.

In both flows under consideration, equilibrium turbulence is perturbed, and a new equilibrium is reached. In both cases the subgrid scales reach the new equilibrium substantially faster than the large, resolved, ones. However, the return to equilibrium of the subgrid scales requires a finite time and is not instantaneous.

From a modeling point of view, this result indicates that SGS models would benefit from incorporating nonequilibrium behavior to predict more accurately engineering flows, in which a variety of effects (pressure gradients, secondary shear, etc.) may act to perturb the canonical flows. An effi-

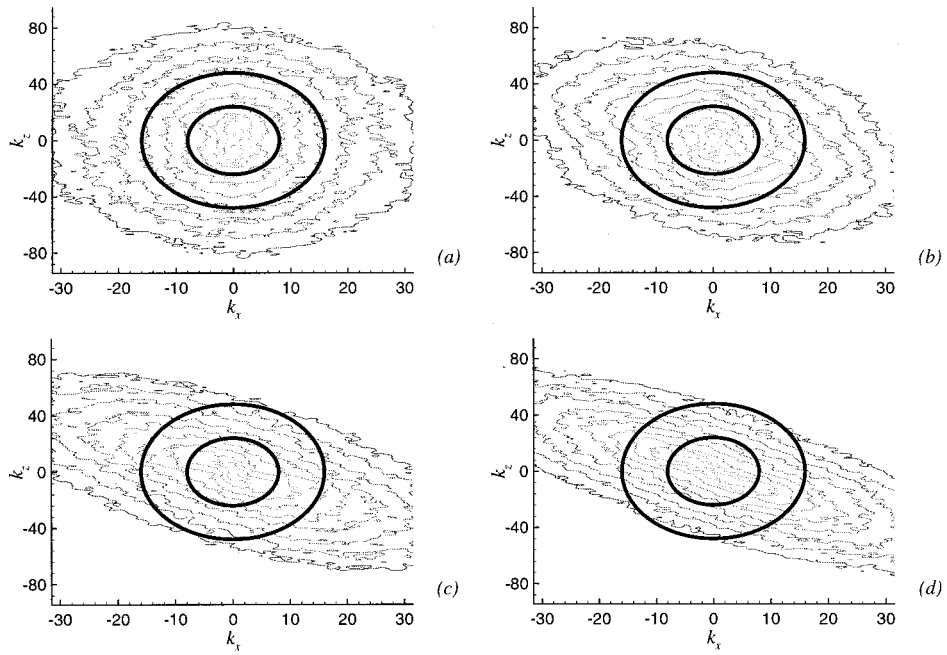

FIG. 14. Kinetic energy spectra (normalized by u_τ) at $y^+=15$. Three-dimensional boundary layer. The contour levels are exponentially spaced between 10^{-7} (black) and 10^0 (grey); the two ellipses roughly correspond to the grid- and test-filter wave numbers. (a) $tu_{\tau,o}/\delta=0$; (b) $tu_{\tau,o}/\delta=0.14$; (c) $tu_{\tau,o}/\delta=0.29$; (d) $tu_{\tau,o}/\delta=0.60$.

cient and inexpensive way to take those effects into account is to use the smallest resolved scales to parametrize the unresolved ones, as is done in scale-similar and dynamic models. These models have been found to respond more accurately to perturbations than models, like the Smagorinsky model, that are mostly affected by the largest scales of motion. The present results further confirm the robustness of dynamic SGS models in computing nonequilibrium flows.

While the dynamic eddy viscosity model predicts the overall levels of energy drained from the large scales quite accurately, scale-similar models are much more effective at representing the correlation between the production of large-

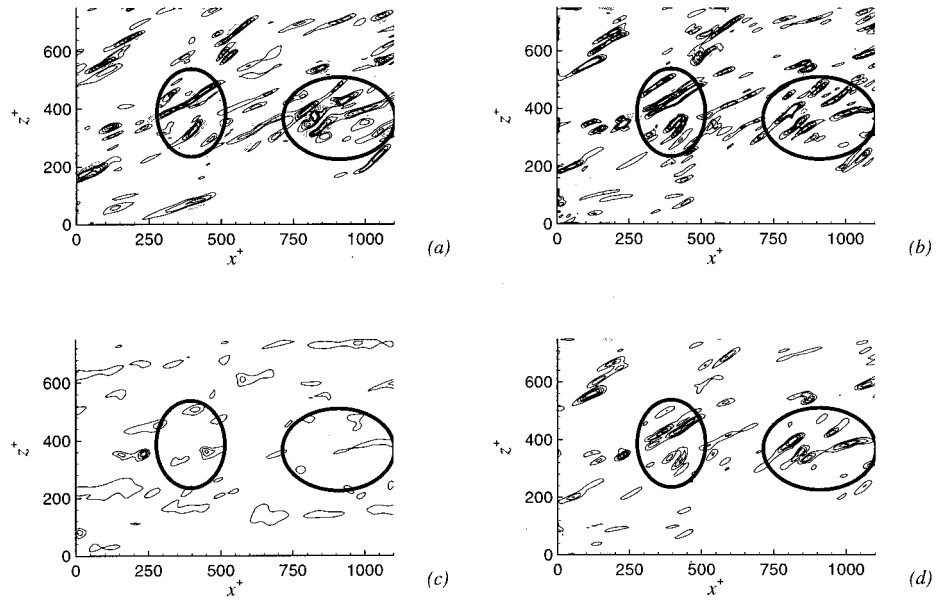

FIG. 15. Spatial distribution of the large-scale and SGS energy production on the $y^+=12$ plane at $tu_{\tau,o}/\delta=0.3$. Three-dimensional boundary layer. Tophat filter, $\Delta_i=2\Delta x_i$. All quantities are normalized by $u_{\tau,o}$ and ν. Positive contours are grey, negative are black. (a) Total production, $u_i'u_j'(\partial U_i/\partial x_j)$; contour level intervals are ± 0.8. (b) Production of SGS energy (exact); contour level intervals are ± 0.06. (c) Production of SGS energy (dynamic eddy-viscosity model[6,7]); contour level intervals are ± 0.06. (d) Production of SGS energy (scale similar model[9]); contour level intervals are ± 0.06. The ellipses highlight regions of significant production.

scale energy and production of SGS energy that has been observed in these nonequilibrium flows, and also in the near-wall region of equilibrium boundary layers.[12] Mixed models, which combine a scale-similar model with a dissipative, eddy-viscosity term, are likely to be very effective parametrizations of the SGS stresses in nonequilibrium flows.

ACKNOWLEDGMENTS

Support for this research was provided by the Office of Naval Research, Grants No. N00014-91-J-1638 (UP) and No. N0014-94-1-0016 (GNC and JK) monitored by Dr. L. Patrick Purtell. Computer time was provided by the Naval Oceanographic Office, the NAS program at NASA–Ames Research Center, and the San Diego Supercomputer Center.

[1]J. Smagorinsky, ''General circulation experiments with the primitive equations. I. The basic experiment,'' Mon. Weather Rev. **91**, 99 (1963).
[2]D. K. Lilly, ''The representation of small-scale turbulence in numerical simulation experiments,'' *Proceedings of the IBM Scientific Computing Symposium on Environmental Sciences*, Yorktown Heights, NY (unpublished).
[3]L. M. Smith and V. Yakhot, ''Short and long-time behavior of eddy viscosity models,'' Theor. Comput. Fluid Dyn. **4**, 197 (1993).
[4]J. Bardina, J. H. Ferziger, and R. S. Rogallo, ''Effect of rotation on isotropic turbulence: Computation and modelling.'' J. Fluid Mech. **154**, 321 (1985).
[5]G. N. Coleman, J. Kim, and A.-T. Le, ''A numerical study of three-dimensional boundary layers,'' *Proceedings of the 10th Turbulent Shear Flow Conference*, State College, PA, 1995 (unpublished).
[6]M. Germano, U. Piomelli, P. Moin, and W. H. Cabot, ''A dynamic subgrid-scale eddy viscosity model,'' Phys. Fluids A **3**, 1760 (1991).
[7]D. K. Lilly, ''A proposed modification of the Germano subgrid-scale closure method,'' Phys. Fluids A **4**, 633 (1992).
[8]J. Bardina, J. H. Ferziger, and W. C. Reynolds, ''Improved subgrid scale models for large eddy simulation,'' AIAA Paper No. 80–1357, 1980.
[9]S. Liu, C. Meneveau, and J. Katz, ''On the properties of similarity subgrid-scale models as deduced from measurements in a turbulent jet,'' J. Fluid Mech. **275**, 83 (1994).
[10]E. R. Van Driest, ''On the turbulent flow near a wall,'' J. Aero. Sci. **23**, 1007 (1956).
[11]U. Piomelli, ''High Reynolds number calculations using the dynamic subgrid-scale stress model,'' Phys. Fluids A **5**, 1484 (1993).
[12]U. Piomelli, Y. Yu, and R. J. Adrian, ''Subgrid-scale energy transfer and near-wall turbulence structure,'' Phys. Fluids **8**, 215 (1996).
[13]J. Kim, P. Moin, and R. D. Moser, ''Turbulence statistics in fully-developed channel flow at low Reynolds number,'' J. Fluid Mech. **177**, 133 (1987).
[14]N. N. Mansour, J. Kim, and P. Moin, ''Reynolds stress and dissipation-rate budgets in a turbulent channel flow,'' J. Fluid Mech. **194**, 15 (1988).
[15]R. H. Kraichnan, ''Eddy viscosity in two and three dimensions,'' J. Atmos. Sci. **33**, 1521 (1976).
[16]J. A. Domaradzki, W. Liu, and M. E. Brachet, ''An analysis of subgrid-scale interactions in numerically simulated isotropic turbulence,'' Phys. Fluids A **5**, 1747 (1993).
[17]J. A. Domaradzki, W. Liu, C. Härtel, and L. Kleiser, ''Energy transfer in numerically simulated wall-bounded turbulent flows,'' Phys. Fluids **6**, 1583 (1994).